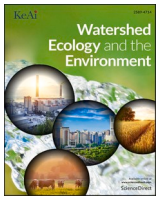
Watershed Ecology and the Environment 7 (2025) 144–158

Contents lists available at ScienceDirect

Watershed Ecology and the Environment

journal homepage: www.keaipublishing.com/en/journals/watershed-ecology



Advancing wetland mapping in Argentina: A probabilistic approach integrating remote sensing, machine learning, and cloud computing towards sustainable ecosystem monitoring

María F. Navarro Rau [a,*], Noelia C. Calamari [b], Carlos S. Navarro [c], Andrea Enriquez [d,r], María J. Mosciaro [e], Griselda Saucedo [f], Raul Barrios [f], Matías Curcio [h], Victorio Dieta [g], Guillermo García Martínez [h], María del R. Iturralde Elortegui [i], Nicole J. Michard [j], Paula Paredes [k], Fernando Umaña [d], Silvina Alday [l], Alejandro Pezzola [m], Claudia Vidal [c], Cristina Winschel [m], Silvia Albarracin Franco [n], Santiago Behr [o], Francisco A. Cianfagna [r], Maria V. Cremona [d], Fernando Alvarenga [n], Ruth Perucca [f], Astor Lopez [p], Federico Miranda [q], Ditmar B. Kurtz [f]

[a] *Instituto de Suelos, Instituto Nacional de Tecnología Agropecuaria (INTA), De los Reseros y Las Cabañas (HB1712WAA), Hurlingham, Buenos Aires, Argentina*
[b] *Estación Experimental Paraná, Instituto Nacional de Tecnología Agropecuaria (INTA), Ruta Nacional 11 km 12.7 (E3100XAD), Oro Verde, Entre Ríos, Argentina*
[c] *Estación Experimental Reconquista, Instituto Nacional de Tecnología Agropecuaria (INTA), Ruta Nacional 11 km 773 (A4403AGE), Reconquista, Santa Fe, Argentina*
[d] *Estación Experimental Bariloche, Instituto Nacional de Tecnología Agropecuaria (INTA), Modesta Victoria 4450 (8400), San Carlos de Bariloche, Río Negro, Argentina*
[e] *Estación Experimental Salta, Instituto Nacional de Tecnología Agropecuaria (INTA), Ruta Nacional 68 km 172 (A4403AGE), Cerrillos, Salta, Argentina*
[f] *Estación Experimental Corrientes, Instituto Nacional de Tecnología Agropecuaria (INTA), Ruta Nacional 12 Km 1008 (3416), Corrientes, Argentina*
[g] *Agencia de Extensión Rural Delta Frontal, Instituto Nacional de Tecnología Agropecuaria (INTA), Las Casuarinas s/n esq. Eucalyptus- Puerto de Frutos (1648), Tigre, Buenos Aires, Argentina*
[h] *Estación Experimental Esquel, Instituto Nacional de Tecnología Agropecuaria (INTA), Chacabuco 513 U9200 Esquel, Chubut, Argentina*
[i] *Agencia de Extensión Olavarría, Instituto Nacional de Tecnología Agropecuaria (INTA), Alsina 2642 (7400), Olavarría, Buenos Aires, Argentina*
[j] *Instituto de Recursos Biológicos, Instituto Nacional de Tecnología Agropecuaria (INTA), De los Reseros y Las Cabañas (HB1712WAA), Hurlingham, Buenos Aires, Argentina*
[k] *Estación Experimental Santa Cruz, Instituto Nacional de Tecnología Agropecuaria (INTA), Mahatma Gandhi N° 1322 (9400), Río Gallegos, Santa Cruz, Argentina*
[l] *Estación Experimental San Juan, Instituto Nacional de Tecnología Agropecuaria (INTA), Calle 11 y Vidart (5427), Villa Aberastain, San Juan, Argentina*
[m] *Estación Experimental Ascasubi, Instituto Nacional de Tecnología Agropecuaria (INTA), Ruta Nacional 3 Km 794 (B8142), Hilario Ascasubi, Buenos Aires, Argentina*
[n] *Estación Experimental Cerro Azul, Instituto Nacional de Tecnología Agropecuaria (INTA), Ruta Nacional 1. Km. 1085 (N 3313), Cerro Azul, Misiones, Argentina*
[o] *Estación Experimental Chubut, Instituto Nacional de Tecnología Agropecuaria (INTA), 25 de Mayo N° 4870 (9100), Trelew, Chubut, Argentina*
[p] *Estación Experimental Saenz Peña, Instituto Nacional de Tecnología Agropecuaria (INTA), Ruta Nacional 95 Km. 1108 (3700), Presidencia Roque Sáenz Peña, Chaco, Argentina*
[q] *Estación Experimental Formosa, Instituto Nacional de Tecnología Agropecuaria (INTA), Av. Carlos Pellegrini s/n (3603), El Colorado, Formosa, Argentina*
[r] *Consejo Nacional de Investigaciones Científicas y Técnicas (CONICET), Argentina*

ARTICLE INFO

Keywords:
Wetland mapping
Google earth engine
Random forest

ABSTRACT

Wetlands, covering 7 % of Earth's surface, are crucial for providing ecosystem services and regulating climate change. Despite their importance, global fluctuations in wetland distribution highlight the need for accurate and comprehensive mapping to address current and future challenges. In Argentina, a lack of detailed knowledge about wetland distribution, extent, and dynamics impedes effective conservation and management efforts. This

* Corresponding author.
E-mail addresses: navarroderau.maria@inta.gob.ar (M.F. Navarro Rau), calamari.noelia@inta.gob.ar (N.C. Calamari), navarro.carlossaul@inta.gob.ar (C.S. Navarro), enriquez.andrea@inta.gob.ar (A. Enriquez), mosciaro.maria@inta.gob.ar (M.J. Mosciaro), saucedo.griselda@inta.gob.ar (G. Saucedo), barrios.raul@inta.gob.ar (R. Barrios), mcurcio@agro.uba.ar (M. Curcio), dieta.victorio@inta.gob.ar (V. Dieta), garcia.guillermo@inta.gob.ar (G.G. Martínez), iturraldeelortegui.m@inta.gob.ar (M.R. Iturralde Elortegui), michard.nicole@inta.gob.ar (N.J. Michard), paredes.paula@inta.gob.ar (P. Paredes), umana.fernando@inta.gob.ar (F. Umaña), alday.silvina@inta.gob.ar (S. Alday), pezzola.alejandro@inta.gob.ar (A. Pezzola), vidal.claudia@inta.gob.ar (C. Vidal), winschel.cristina@inta.gob.ar (C. Winschel), albarracin.silvia@inta.gob.ar (S.A. Franco), behr.santiago@inta.gob.ar (S. Behr), francianfagna@gmail.com (F.A. Cianfagna), cremona.mv@inta.gob.ar (M.V. Cremona), alvarenga.fernando@inta.gob.ar (F. Alvarenga), perucca.alba@inta.gob.ar (R. Perucca), lopez.astor@inta.gob.ar (A. Lopez), mirando.federico@inta.gob.ar (F. Miranda), kurtz.ditmar@inta.gob.ar (D.B. Kurtz).

https://doi.org/10.1016/j.wsee.2025.04.001
Received 20 August 2024; Received in revised form 31 March 2025; Accepted 1 April 2025
Available online 4 April 2025
2589-4714/© 2025 The Authors. Publishing services by Elsevier B.V. on behalf of KeAi Communications Co. Ltd. This is an open access article under the CC BY license (http://creativecommons.org/licenses/by/4.0/).

Remote sensing
Wetland dynamic
Biophysical indices
Probabilistic modeling
Argentina

study addresses these challenges by presenting a probabilistic wetland distribution map for Argentina, integrating 20 years of satellite imagery with machine learning and cloud computing technologies. Our approach introduces a comprehensive set of biophysical indices, enabling the identification of key wetland characteristics: 1) permanent or temporal surface water presence; 2) water-adapted vegetation phenology; and 3) geomorphology conducive to water accumulation. Our model achieved an accuracy of 89.3 %, effectively identifying wetland areas and delineating "elasticity" zones that reveal temporal wetland behavior. Approximately 9.5 % of Argentina is classified as wetlands, with the Chaco-Mesopotamia region accounting for 43 % of these areas. The performance of the 42 assessed variables varied across macro-regions, highlighting the necessity for region-specific classification methods. In the Andean region, variables such as the Digital Elevation Model (DEM) and Topographic Wetness Index (TWI) were key predictors, while in the plains, spectral properties including vegetation and water content indices were more significant. Despite challenges in classifying irrigated areas, the model demonstrated considerable robustness. This study not only enhances our understanding of wetland dynamics but also provides insights into how different regions respond to various environmental factors, offering a more nuanced perspective on wetland behavior. These findings pave the way for refined conservation strategies and further research into the impacts of climate change and land use on wetland ecosystems. The precision, scalability, and representation of wetland elasticity emphasize its importance for decision-making and provide a crucial baseline for future research amid ongoing environmental changes.

Introduction

Wetlands, though covering only about 7 % of the Earth's surface, are essential ecosystems characterized by the presence of water, either permanent or temporary (Ramsar Convention on Wetlands, 2018). Despite their limited spatial extent, wetlands are critical ecosystems that provide multiples and essential services such as water purification and storage, natural hazard mitigation, soil and water conservation, flood control, and shoreline protection (Mitsch and Gosselink, 2015; Marton et al., 2015; Aslam et al., 2023). Wetlands are also global hotspots of biological diversity (Junk et al., 2013), support fish and agricultural products, and are key contributors to sediment retention and carbon sequestration (Mitsch et al., 2013; Tiner et al., 2015; Kingsford et al., 2016), playing a key role in climate change regulation and mitigation (Gumbricht et al., 2017; Aslam et al., 2024a).

Notwithstanding their significance, the reported global distribution of wetlands still exhibits variability due to factors such as classification criteria, field survey methodologies, and estimation approaches (Tiner et al., 2015). As Davidson and Finlayson (2018) highlights, understanding the extent and regional distribution of wetlands is crucial for addressing these variabilities. Consequently, there is a pressing need to redirect efforts toward generating a more accurate wetland distribution map that reflects the pressures these ecosystems currently face and will encounter in the future.

Despite their benefits, wetlands are continuously threatened from human activities, such as urbanization, agriculture, and climate change, leading to accelerated degradation, particularly in South America (Junk et al., 2013; Davidson, 2014; Gardner et al., 2015; Mahdavi et al., 2018; Darrah et al., 2019; Neiff, 2021). Although global wetland losses have been reported (Fluet-Chouinard et al., 2023), the lack of accurate wetland maps introduces errors in those estimations, making robust quantification crucial for identifying conservation priorities and guiding sustainable management strategies (Gabrielsen et al., 2016).

A wetland distribution map is valuable, but a real-time environmental monitoring system is essential (Souza et al., 2019; Eid et al., 2020; Shafi et al., 2023). Remotely sensed data provides a cost-effective solution for wetland classification across large areas, improving accuracy and enabling long-term monitoring through multi-temporal satellite images (Fournier et al., 2007; Mahdavi et al., 2018; Amani et al., 2019; DeLancey et al., 2019). This approach is crucial for tracking dynamic changes in wetlands, particularly in response to climatic events like El Niño and La Niña, which can significantly alter wetland surface areas (Pandey et al., 2017; Ilyas et al., 2019; Cai et al., 2020). New technologies and low-cost solutions enhance the processing of extensive geographical data, benefiting nations with limited resources. For accurate national wetland quantification, high-quality remotely sensed imagery free from disturbances such as clouds, haze, and shadows is essential (Mahdianpari et al., 2018).

Probabilistic determination of wetland distribution improves traditional classification methods, though it has been applied to wetland mapping in only a few studies (Humphreys et al., 2017; DeLancey et al., 2019; Shafi et al., 2023). In this context, advanced cloud-based frameworks, such as Google Earth Engine (GEE), combined with open-access information and machine learning tools like Random Forest (RF), provide unprecedented opportunities for large-scale wetland mapping (Gorelick et al., 2017; DeLancey et al., 2019; Amani et al., 2019). Recent advancements in machine learning have significantly enhanced wetland mapping by enabling the development of accurate and detailed maps (Mallick et al., 2021; Aslam et al., 2024b). Techniques such as convolutional neural networks and deep learning have been successfully employed to classify wetland habitats across various ecosystems (Jafarzadeh et al., 2022; Mainali et al., 2023). By integrating these methods with open-source tools and publicly available datasets, wetland mapping has become more accessible, providing valuable insights for conservation and land management practices, especially amidst environmental changes (Gemechu et al., 2021; Mallick et al., 2021).

Since 2013, the debate over federal legislation to regulate wetlands in Argentina has been ongoing, with numerous proposals but still no consensus reached. In this context, having reliable information on wetland distribution and extent is crucial for effective management. Although valuable studies conducted in Argentina have provided insights into wetland distribution (Fabricante et al., 2022; Kandus et al., 2008; Canevari et al., 1999), variations in datasets, methodologies, and definitions have led to discrepancies in estimates, complicating comparisons. This underscores the need for a unified approach to wetland mapping and management, addressing negative impacts more effectively (Pereira et al., 2023). An accurate national wetland distribution map is vital for understanding ecosystem conditions, conserving biodiversity, and monitoring changes (Melendez-Pastor et al., 2010; Mao et al., 2020; Qu et al., 2023). Our study aims to tackle these challenges by employing multi-temporal satellite imagery, cloud computing, and machine learning algorithms. By integrating a range of biophysical variables and adopting a probabilistic approach, we will produce a reliable and up-to-date national wetland map for Argentina, enabling the visualization of wetland dynamics across different phases of water supply, such as El Niño and La Niña.

Materials and methods

Study area

This study was conducted in Argentina, a vast and diverse country covering nearly 2.8 million km^2. The climate in Argentina varies widely, ranging from sub-Antarctic conditions in the southern regions to warm

subtropical climates in the northern areas, and from humid conditions in the eastern parts to arid conditions in the western regions. Annual rainfall varies significantly, ranging from approximately 40 to 4000 mm yr^{-1}. Mean maximum and minimum temperatures range from approximately 35.5 °C in the warmest months, to −6°C in the coldest months (available in: https://www.smn.gob.ar/descarga-de-datos).

Argentina features diverse ecosystems, including grasslands, steppes, forests, croplands, meadows, and wetlands distributed across the country. The distribution of wetlands is strongly influenced by precipitation patterns throughout the region due to extensive latitudinal and longitudinal gradients, diverse climate, and hydro-geomorphological features. As a result, wetland regions have been recently classified (Benzaquén et al., 2017) (Fig. 1).

Overall framework

The Ramsar Convention on Wetlands (Convention, 1971) adopted a comprehensive definition encompassing nearly all wetland types: 'areas of marsh, fen, peatland, or water—natural or artificial, permanent or temporary, with static or flowing water, whether fresh, brackish, or salt, including marine areas not exceeding six meters in depth at low tide. However, the wetland criteria designed for field use are impractical for large-scale mapping, as evidenced by the wide range of area estimates across various studies (Mahdavi et al., 2018). In this study, we use the technical definition of wetlands proposed by Ministerial Resolution 329 (2016) of the Federal Environment Council of Argentina: wetlands are environments where surface or subsurface water, whether temporary or permanent, causes biogeochemical changes compared to terrestrial and aquatic environments. Key features include the adapted biota, often hydrophytic plants, and/or waterlogged soils or substrates (non-soils) with hydromorphic traits.

Wetlands display a spatio-temporal dynamic pattern, often described as elasticity. Neiff et al. (1994) defined elasticity as the ratio between the areas occupied during maximum flooding and areas occupied during

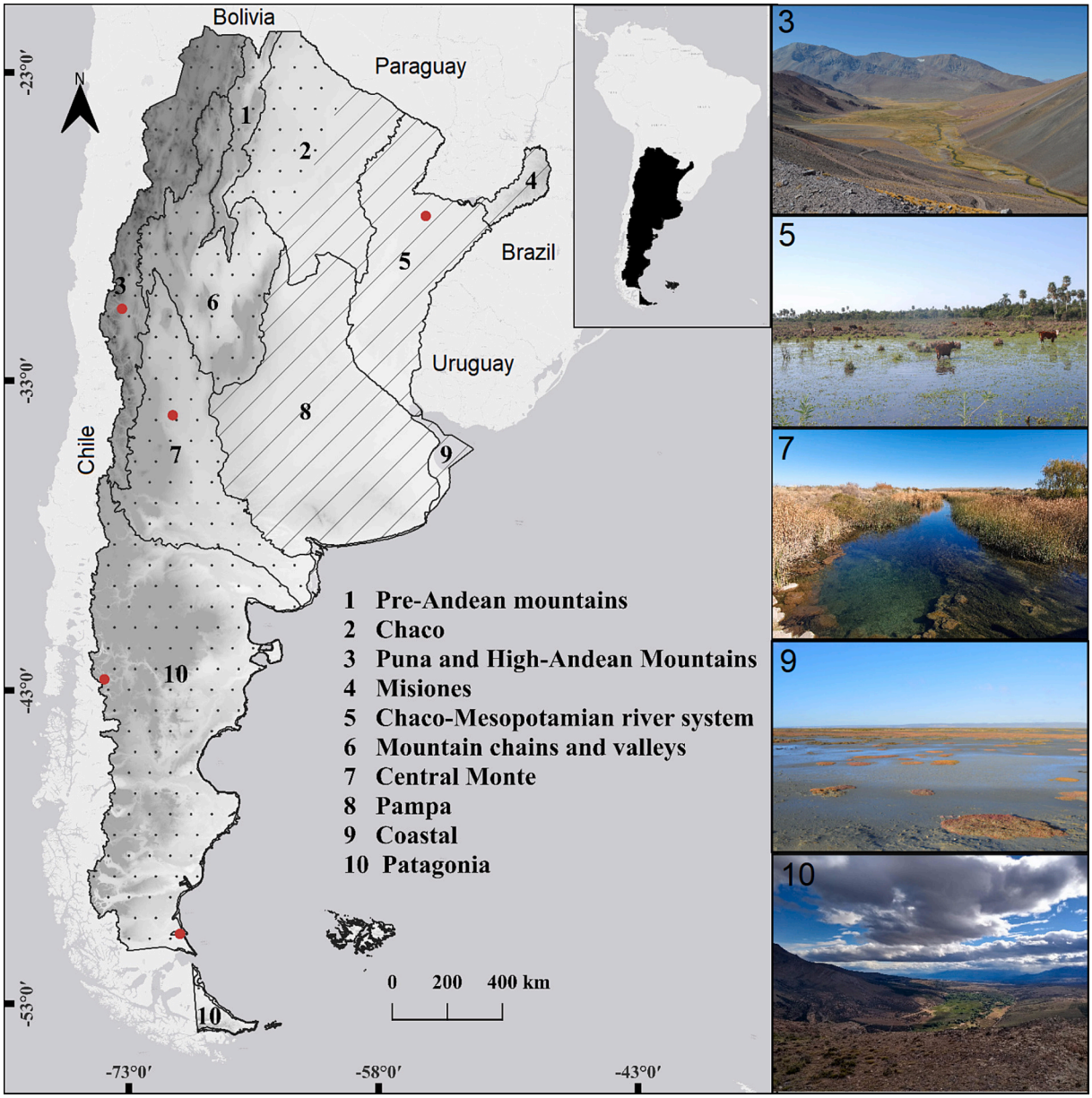


Fig. 1. Argentina's wetland regions (based on Benzaquén et al., 2017). The patterns indicate the Andean and extra-Andean arid/semi-arid (dots) and the humid/sub-humid plains (stripes). The images showcase examples of representative wetlands in different regions (from top to bottom: regions 3, 5, 7, 9 and 10, locations indicated by red dots). (For interpretation of the references to colour in this figure legend, the reader is referred to the web version of this article.)

maximum drought. These fluctuations are influenced by natural wet and dry cycles, climate variability, and extreme weather events like El Niño. Factors such as geomorphology, soil composition, vegetation, climate, and land use shape this pattern (Jackson, 2014). To manage this complexity, we use a probabilistic approach integrating: 1) permanent or temporal surface water presence; 2) water-adapted vegetation phenology; and 3) hydro-geomorphological characteristics based on topographic data.

The study unfolds through several key stages: i) data acquisition and pre-processing, ii) identification of optimal classification features, iii) supervised classification, and iv) classification accuracy assessment (Fig. 2).

Data acquisition and preprocessing

Training and reference data. For the classification, we used the JRC Global Surface Water dataset, Landsat images, the SRTM-ALOS Digital Elevation Model (included in the MDE-Ar 2.1 product), and additional ancillary data (Table 1). Landsat 5 TM and Landsat 8 OLI images were selected, covering the entire study area from Path 223 to 233 (east to west) and Row 75 to 98 (north to south), with three additional scenes for Islas Malvinas. Landsat 5 was used for its historical data, providing valuable insights into long-term changes, while Landsat 8 was included to ensure high-quality imagery for more recent years. By combining Landsat 5 and Landsat 8, we ensured both the continuity and quality of the dataset throughout the analysis period (2000–2020), thereby enhancing the robustness of our findings (Table 1). Although Landsat 7 provides more recent data, it was excluded from the analysis due to the failure of its scan line corrector, which compromises data reliability.

A dataset of 26,000 points was randomly distributed across two strata. One stratum, representing 30 % of the dataset, included stream, river, and other water body polygons from ancillary sources (Table 1). The remaining 70 % of the points were distributed uniformly across the rest of the area. Standardization involved placing one point every 100 km^2 with a minimum of 1 km separation. We used the Collect Earth Desktop tool (CE) (Bey et al., 2016) for consistent reference data,

Table 1
Datasets used in this study.

Name	Summary	Spatial Resolution	Date	Source
Landsat 5 TM	USGS Landsat 5 TM Collection 1 Tier 1 calibrated top-of-atmosphere (TOA) Reflectance	30 *m*	2000—2013	Courtesy of the U.S. Geological Survey
Landsat 8 OLI	USGS Landsat 8 OLI Collection 1 Tier 1 TOA reflectance	30 *m*	2014—2020	Courtesy of the U.S. Geological Survey
MDE-Ar 2.1	Provided by the National Geographic Institute (IGN)	30 *m*	2021	https://www.ign.gob.ar/categoria/temática/geodesia/mde-ar
JRC	JRC Global Surface Water Mapping Layers, v1.4	30 *m*	1984—2021	EC JRC/Google (Pekel et al., 2016)
Ancillary Data	Body water (permanent and temporary); urban settlements	Vector Data	2021	https://www.ign.gob.ar/NuestrasActividades/InformacionGeoespacial/CapasSIG

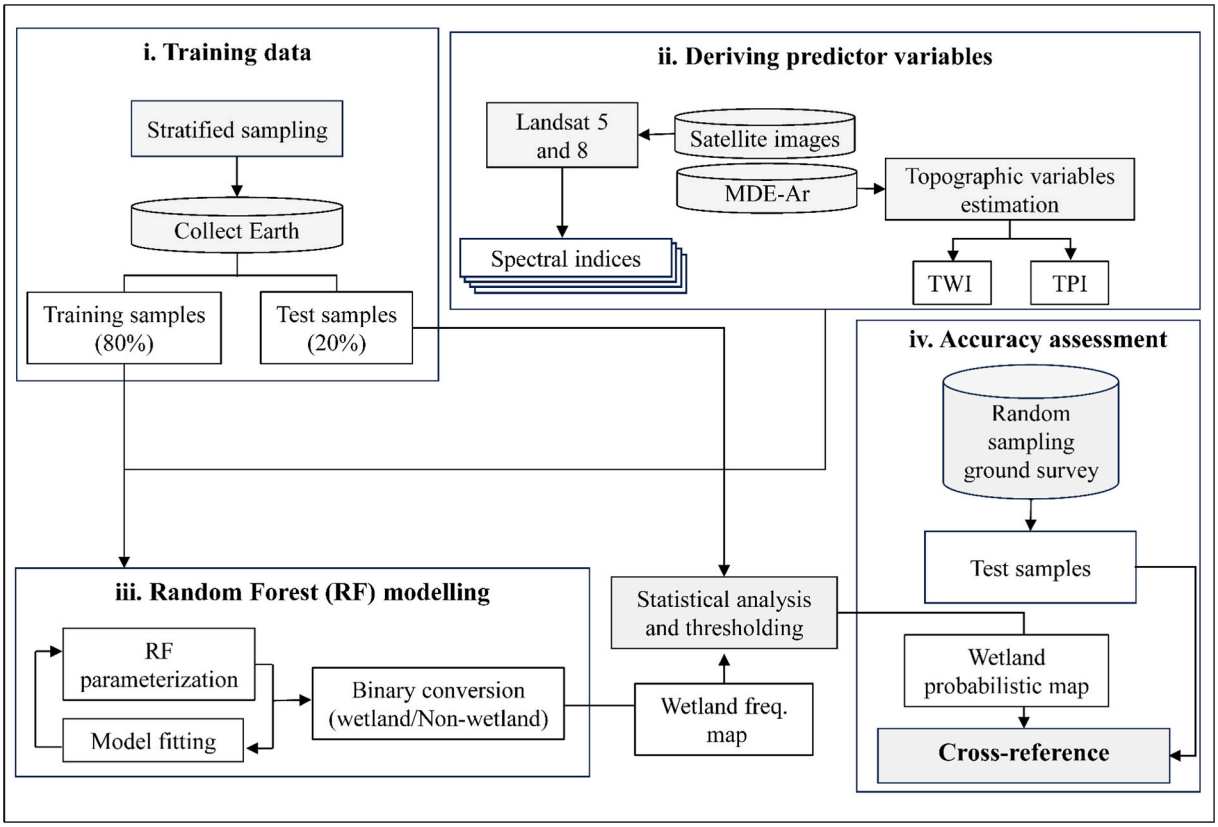


Fig. 2. Workflow diagram of the multi-temporal modeling framework for the probabilistic wetland mapping.

facilitating geosynchronous visualization and analysis of satellite imagery from sources like Google Earth, Bing Maps, and Google Earth Engine. The analysis involved visual interpretation of high and very high-resolution images and vegetation indices such as NDVI. A structured survey template was developed for CE (see Appendix, Fig. A.1), covering various land covers in the country, based on expert delineation and a 0.50 ha plot with a 5x5 point grid. This 20-year analysis considered sample purity, stability, and reliability (Appendix, Fig. A.2). Recognizing rice fields as artificial wetlands (Convention, 2012; Natuhara, 2013; Watanabe, 2018; Zhuang et al., 2020) and their prevalence in areas transformed from natural wetlands for rice production in Argentina, we classified rice fields within the broader wetland category.

Data collection and preprocessing. The national wetland map was created using the GEE platform (Gorelick et al., 2017). To enhance classification accuracy, we integrated multi-temporal images (Amani et al., 2019) from Landsat 5 TM and Landsat 8 OLI, which provide medium-resolution (30 m) and 16-day temporal frequency imagery (Table 1). We chose Landsat remote sensing products for their extensive temporal coverage and open-access accessibility in the GEE catalog, which already include radiometric and atmospheric calibration. (Chander et al., 2009; Hird et al., 2017).

Given the dynamic nature of wetlands due to seasonal water level changes (Devranche et al., 2013; Gxokwe et al., 2020), we used images from the season with the highest water supply, influenced by rainfall or thawings. Our classification used bands 2 to 5 and band 7 from Landsat 5, as well as bands 3 to 7 from Landsat 8, encompassing visible spectrum, Near Infrared (NIR), and Shortwave Infrared (SWIR) channels. Furthermore, we applied cloud and snow masking using Landsat band quality assessment (BQA = 672 and BQA = 2720 for Landsat 5 and Landsat 8, respectively), with a threshold of < 10 % to create a cloud and snow-free composite image.

We extracted four spectral indices sensitive to vegetation, water, and wetness from Landsat 5 and Landsat 8 images, including 1) NDVI (Townshend and Justice, 1986), 2) SAVI (Huete, 1988), 3) NDWI (Gao, 1996), and 4) MNDWI (Xu, 2006). The equations of these indices are as follows (1 to 4, respectively):

$$NDVI = \frac{NIR - Red}{NIR + Red} \tag{1}$$

$$SAVI = \frac{NIR - Red}{NIR + Red + 0.5} * 1.5 \tag{2}$$

$$NDWI = \frac{NIR - SWIR}{NIR + SWIR} \tag{3}$$

$$MNDWI = \frac{Green - SWIR}{Green + SWIR} \tag{4}$$

The rationale for selecting different indices is well documented. We selected the NDVI index for its ability to provide insights into vegetation conditions, its relation to photosynthetically active biomass, and its phenological dynamics (Adam et al., 2010). The SAVI index has been used previously to map and monitor wetland conditions (Eid et al., 2020). Conversely, the NDWI index effectively distinguished land from water cover (Tang et al., 2016), while the MNDWI has been employed in delineating water body boundaries (Du et al., 2016). Both indexes range from -1 to $+1$, with values higher than zero indicating open water areas, and values close to zero indicating areas with high moisture content. Both indices were estimated for the SWIR1 and SWIR2 bands. Additionally, we included the ratio between the Green and NIR bands (R35), in which water has the highest and lowest reflectance, respectively. We generated statistical features, including median, mean, and standard deviation, for each spectral index, which were then used as predictors in the model (Appendix, Table A.1).

Considering the influence of terrain characteristics on the location and extent of wetlands, as well as on the hydrological processes in the landscape (Moore et al., 1991; Gómez-Plaza et al., 2000; Branton and Robinson, 2019), we derived two additional variables from the MDE-Ar. his digital elevation model (DEM), developed by the National Geographic Institute (IGN), has a spatial resolution of 30 m and a vertical accuracy of approximately 2 m, and was created from a combination of data captured by the Shuttle Radar Topography Mission (SRTM) and Advanced Land Observing Satellite (ALOS) missions. Using the System for Automated Geoscientific Analyses open-source software (SAGA; Conrad et al., 2015): the Topographic Wetness Index (TWI) and the Topographic Position Index (TPI), (Table 1). The TWI is a proxy for soil moisture content at a pixel level (Beven and Kirkby, 1979). It allows the identification of areas prone to water accumulation, a characteristic associated with the presence and extent of wetlands (Hird et al., 2017). On the other hand, the TPI provides insights on the elevation of each pixel in relation to its neighboring pixels (De Reu et al., 2013).

$$TWI = \ln\left(\frac{A}{\tan\alpha}\right) \tag{5}$$

$$TPI(x,y) = Z(x,y) - mean(Z) \tag{6}$$

where A is the catchment area (in units of surface area) draining to a specific point, typically derived from a Digital Elevation Model (DEM), α is the slope angle at the point of interest, which can be calculated from the DEM, Z(x,y) is the elevation of the pixel at position (x,y), and mean (Z) is the average elevation of the pixels within a defined neighborhood around (x,y).

To evaluate and detect surface water, we relied on the JRC Global Surface Water dataset, developed under the Copernicus program. This project maps surface water changes globally at a spatial resolution of 30 m using Landsat images. It provides critical information through the bands of stationery, recurrence, and the occurrence of water bodies. We used a total of 42 variables as predictors in the model, which included the described indices and the original bands along with their statistical features (mean, median and standard deviation) (Appendix, Table A.1).

Model fitting and accuracy assessment

For the processing and classification of our extensive dataset comprising 54,720 Landsat images, we selected the Random Forest (RF) algorithm. This choice was based on its robustness and capability to handle high-dimensional data, which are critical for accurate wetland classification in Argentina's diverse landscape. We conducted extensive preliminary analyses across six out of ten regions, testing the performance of several models, including Classification and Regression Trees (CART), Support Vector Machines (SVM), Maximum Entropy (MaxEnt), and RF. SVM and MaxEnt exhibited lower performance with greater variability, with MaxEnt being the weakest performer. While both CART and RF showed strong performance in terms of Overall Accuracy and Kappa Index, CART achieved slightly higher central values. However, CART also showed greater variability in its results, indicating higher sensitivity to data fluctuations. In contrast, RF displayed more consistent and stable performance across regions, making it the most robust and reliable classifier for this study (Appendix, Fig. A.3).

The RF algorithm is an ensemble learning method that constructs a multitude of decision trees during training and outputs the mode of their classes for classification tasks (Breiman, 2001). It employs bootstrap aggregating (or bagging) to create diverse subsets of the training data, which helps to reduce overfitting. Each tree is built on a random sample of the data, and during the splitting process, a random subset of features is considered at each node. This randomness helps to decorrelate the trees, resulting in a more stable and accurate model. Notably, unlike other machine learning models, such as Support Vector Machines or Neural Networks, RF does not require prior normalization of the data and is less prone to overfitting, making it particularly well-suited for our analysis. RF is especially effective for remote sensing applications

because it can manage complex interactions among predictor variables while providing an estimate of variable importance (Whiteside and Bartolo, 2015; Amani et al., 2017; Berhane et al., 2018; Mahdianpari et al., 2018; Simioni et al., 2020, Aslam et al., 2024b).

Parameter configuration

The effectiveness of the RF algorithm relies on several key configuration parameters, which we meticulously tuned based on our preliminary analyses:

- **Number of Decision Trees**: We ultimately set this parameter to **100** after extensive testing. By running the model multiple times across different test regions, we observed that increasing the number of trees beyond this point did not significantly improve accuracy, leading us to conclude that 100 trees would provide a robust and efficient model.
- **Number of Variables for Node Splitting**: Similarly, we selected **5** variables at each split. This decision was based on the performance observed during the preliminary tests, ensuring that each tree adequately represented wetland characteristics while maintaining diversity.
- **Minimum Size of a Terminal Node**: We configured this parameter at **5** to prevent overfitting, as determined through our initial analyses. A larger size enhances the model's ability to generalize across various landscapes.
- **Fraction of Input Data for Bagging**: A value of **0.5** was used, indicating that each tree is built from half of the training data. This method promotes model randomness and mitigates overfitting.
- **Number of Random Seeds**: We employed **5 seeds** to ensure reproducibility of results and stability of the model against random variations in the data.

Additionally, to assess the relative importance of each predictor variable, we segmented the country into two macro-regions: i) the arid and semi-arid Andean region, and ii) the humid and sub-humid plains region. This approach allowed us to better understand how varying environmental conditions influence wetland classification and the relevance of the selected variables.

In summary, the choice of the Random Forest algorithm, alongside the careful optimization of its parameters informed by extensive testing, was fundamental to the success of our wetland mapping analysis, ensuring a balanced approach between accuracy, robustness, and generalization capability.

We utilized the True Skill Statistic (TSS), also known as Hanssen-Kuipers discriminant, to determine the threshold for wetland/non-wetland classification, following Hird et al. (2017). The TSS was computed for different potential classification thresholds (e.g., 0.05, 0.1, 0.15,…,0.85, 0.90, 0.95), and a specific threshold was selected. The TSS is calculated as follows:

$$TSS = Sensitivity + Specificity - 1 \quad (5)$$

where *Sensitivity* represents the producer's accuracy for the wetland class, and *Specificity* represents the producer's accuracy for the non-wetland class.

To convert the frequency values from decision tree votes to probabilities, we employed binary logistic regression, where the presence/absence of wetlands was the independent variable, and frequency values as the explanatory variable. This conversion allowed for more precise classification by representing the likelihood of wetland occurrence as probabilities rather than raw frequencies.

For accuracy assessment, we first compared our results visually with high-resolution multi-temporal images from Google Earth to evaluate how well the classification matched actual ground features. We then cross-referenced our classification with approximately 6,000 ground truth points collected across the study area, ensuring a balanced dataset with a similar number of samples for wetlands and non-wetlands; 30 % of which were provided by other researchers (Oliva et al., 2020; Gaitán et al., 2021). Given this balanced dataset, we chose to utilize accuracy (Accuracy) as our primary metric for model evaluation, as it is more appropriate in contexts where class distributions are even, rather than opting for metrics better suited for imbalanced datasets. We generated an error matrix to evaluate producer, user, and overall accuracies, as well as the kappa coefficient. Verification involved confirming at least one of three wetland components: water, adapted biota, and/or hydric soils (Fig. 3, and Appendix, Fig. A.4), highlighting the rigorous fieldwork undertaken for validation.

Results

The RF model revealed differences in the variables affecting wetland occurrence across macro-regions. In the Andean region, DEM and TWI were key predictors, highlighting the role of terrain characteristics due to the region's rugged topography. Standard deviation measures of spectral indices R35, SAVI, and NDWI2, demonstrated the impact of landscape variability on wetland identification, reflecting terrain complexity (Fig. 4). In contrast, the plains region emphasized spectral characteristics such as band ratios and vegetation and water content indices. Notably, the mean and median values for R35 and Landsat B3 (Green), along with SAVI_stdDev and NDWI2_stdDev, were also relevant (Fig. 4). This region showed less influence from topographic features and a greater emphasis on vegetation and land cover differences. These findings stress the need to tailor classification methods to regional characteristics for improved wetland mapping. Although only the most relevant variables are shown in Fig. 4 for clarity, it is important to note that all 42 predictor variables were included in the RF model, which allows for the inclusion of all variables without a selection process, even in the presence of correlations.

By plotting the TSS, Sensitivity, and Specificity values of the model against various classification thresholds, we chose a wetland frequency of 0.5 to distinguish wetlands from non-wetlands. This threshold corresponded to the point where TSS reached its maximum value and was closely aligned with the balance point of sensitivity and specificity (Fig. 5).

By using the frequency threshold of 0.5, we identified three distinct zones: i) Non-wetlands, with frequency values below 0.5; ii) Wetland elasticity zones, with values ranging from 0.5 to 0.7; and iii) Wetlands, where characteristics are clearly expressed, with frequency values above 0.7 (Fig. 6).

The logistic regression model yielded Argentina's long-term probabilistic wetland distribution map, using a threshold probability of 0.7, with a significant p-value $\leq$ 0.0001 and an AUC of 0.936 (Appendix, Fig. A.5). Based on this threshold, we reclassified the continuous probability values into three ranges: values $<$ 0.7 indicate non-wetlands, while values $\geq$ 0.7 were further divided into two ranges: 0.7–0.8, which represents the wetland elasticity area, and 0.8–1.0, corresponding to the core wetland area (Fig. 7).

According to our estimates, approximately 9.5 % (over 250,000 km2) of Argentina's land area is covered by wetlands (Fig. 7; Table 2). Of these, 1 % (30,500 km2) falls within the 0.70–0.80 probability range, identified as the wetland elasticity zone; 8.5 % (234,800 km2) falls within the 0.80–1.0 range (Table 2). The Chaco-Mesopotamian river system is the largest wetland region, covering approximately 43 % (107,000 km2) of the total wetland area.

Most wetlands were found in the humid and sub-humid regions, with around 81 % of the total wetlands. Whereas arid and semi-arid regions accounted for 14 % of the wetlands, and coastal areas for 5 % along the Argentinean Sea.

Four enlarged sections of these maps, along with the corresponding high-resolution images, are displayed in Fig. 8 for visual assessment. Upon visual inspection, most of the classified areas appear to be faithful representations of reality. Notably, comparison with high-resolution global imagery base maps available in QGIS shows that rivers,

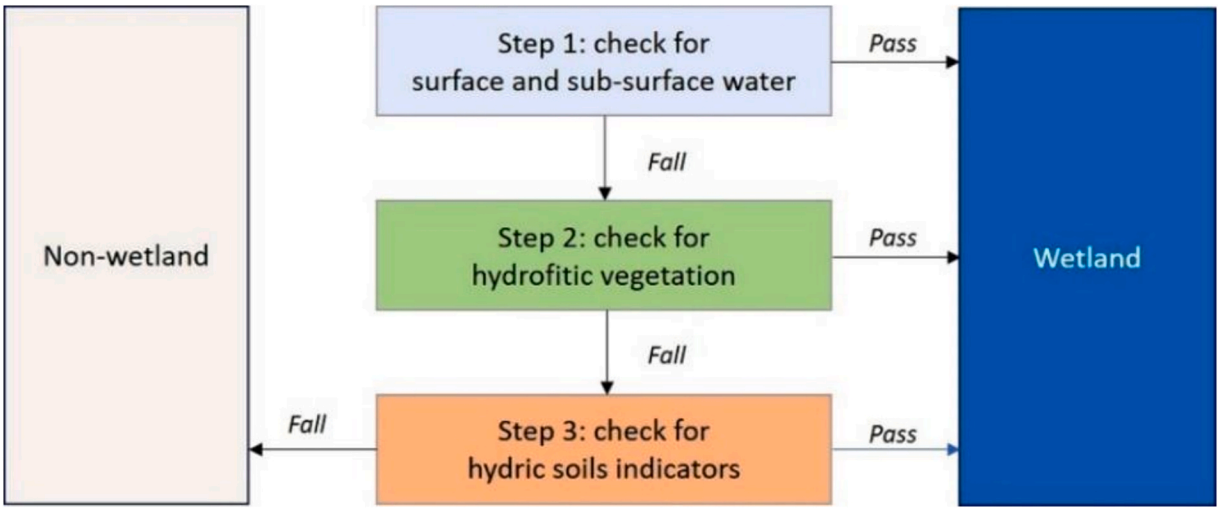


Fig. 3. Sequential workflow wetland confirmation.

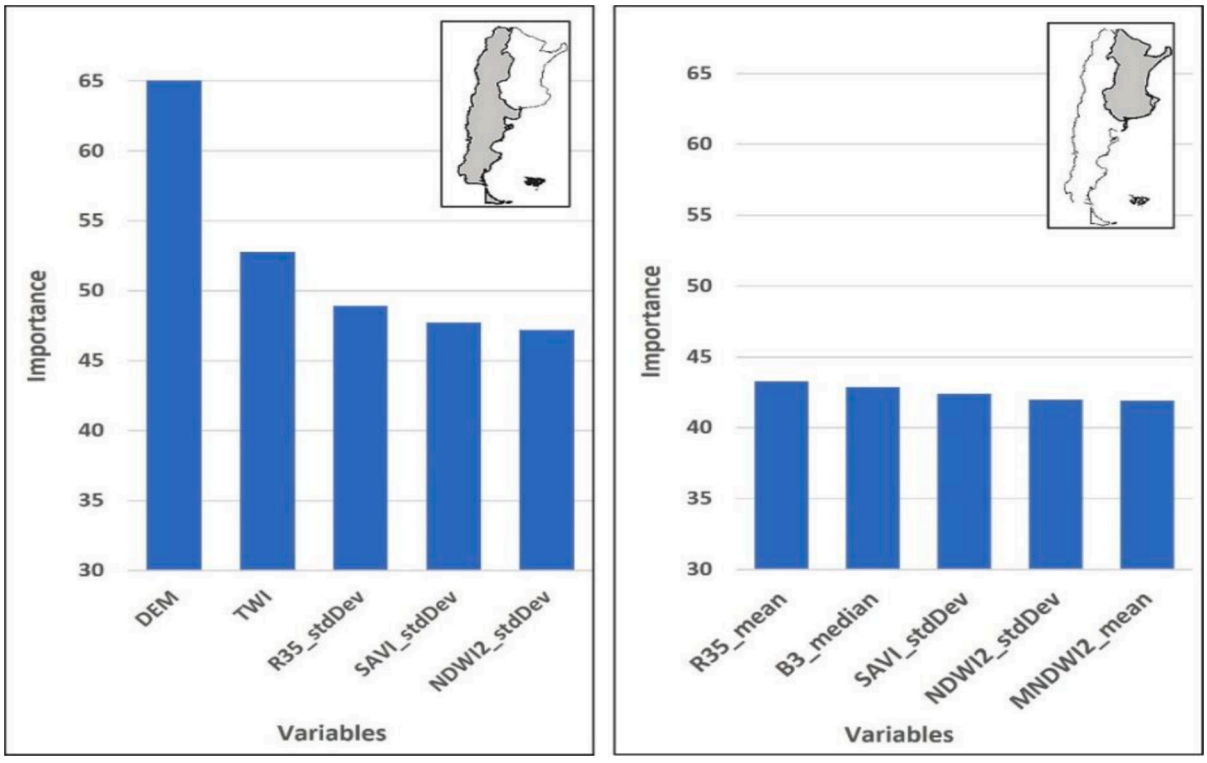


Fig. 4. Importance of the top five predictor variables of the Random Forest model (excerpt from all variables). Andean and extra-Andean arid/semi-arid (on the left), and humid/sub-humid plains regions (on the right). Where, DEM = digital elevation model; TWI = topographic wetness index; R35_stdDev = standard deviation of the Band 3 / Band 5 ratio; SAVI_stdDev = standard deviation of the soil adjusted vegetation index; NDWI2_stdDev = standard deviation of the normalized difference water index from SWIR2; R35_mean = arithmetic mean of the Band 3 / Band 5 ratio; R3_median = arithmetic median of Band 3 values; MNDWI2_mean = arithmetic mean of the modified normalized difference water index from SWIR2.

streams, and water bodies are well-represented (Fig. 8a and b) Similarly, areas surrounding marshes, rivers, streams, and water bodies were appropriately categorized as wetland elasticity zones, showing probability values between 0.7 and 0.8 (Fig. 8b and c).

Our model achieved 89.3 % accuracy (0.72 kappa statistic) with a 0.7 threshold. For the wetland class, producer and user accuracies were 94 %, while the accuracy for the non-wetlands class was 85 %. The most challenging aspect of this classification included overestimating wetlands in flood-irrigated fields in arid and semi-arid regions (Fig. 9a), and misclassifications involving roads bordered by water and vegetation on one or both sides (Fig. 9b).

Discussion

Our research substantially advances the understanding of wetland dynamics by providing a detailed and accurate representation of wetland distribution in Argentina. By leveraging machine learning algorithms applied to multi-temporal satellite imagery from the GEE platform, along with a comprehensive set of biophysical variables, we effectively captured the key characteristics of wetlands. This approach

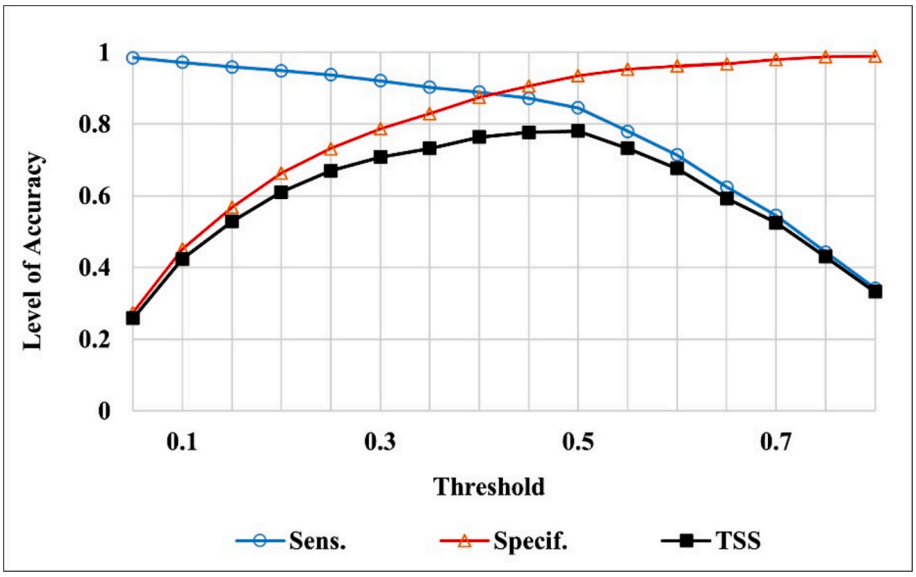


Fig. 5. True Skill Statistic (TSS), Sensitivity, and Specificity values plotted over a classification threshold for the model. Dotted vertical line indicates the threshold value for wetland occurrence.

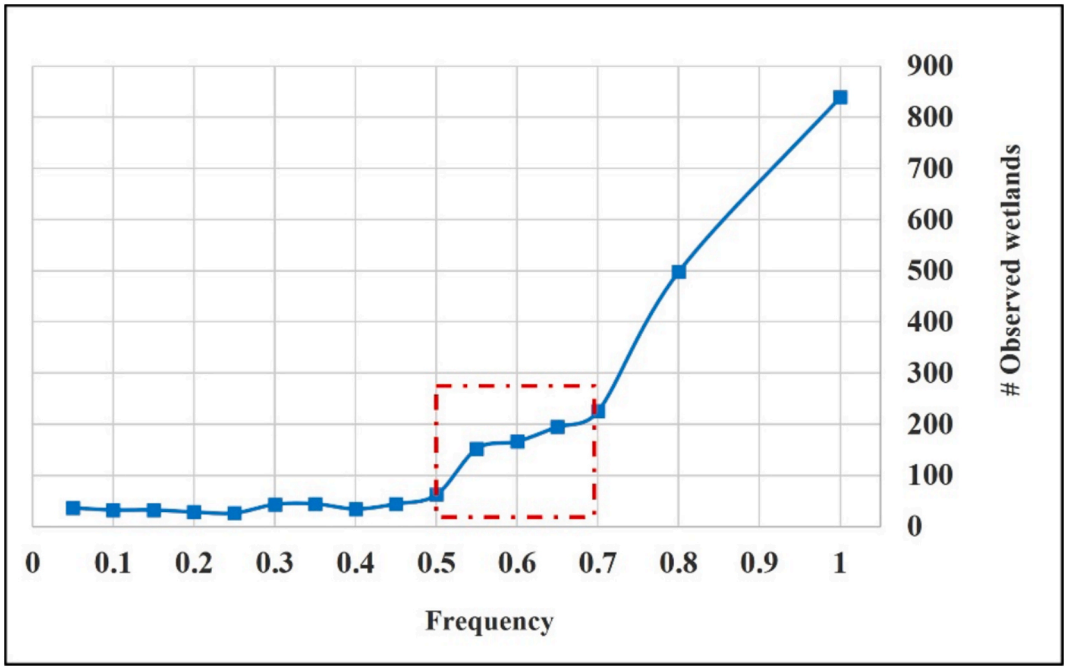


Fig. 6. Relationship between the frequency values obtained by the classification model and the observed values. The red square indicates the values corresponding to the wetland elasticity zone. (For interpretation of the references to colour in this figure legend, the reader is referred to the web version of this article.)

proved robust for creating a high-accuracy probabilistic wetland map of Argentina, accommodating the country's diverse geomorphological and climatic conditions. Our methodology demonstrated flexibility, accurately mapping across various environments, from the challenging Andean highlands to the extensive lowlands, by integrating a wide range of predictor variables. This not only enhances our understanding of wetland spatial patterns but also provides valuable regional insights, such as the prominence of the Chaco-Mesopotamian river system. Our findings are consistent with other studies that used diverse data sources to wetland and land cover predictions (Mellor et al., 2013; Maxwell et al., 2016; Hird et al., 2017; DeLancey et al., 2019; Aslam et al., 2024b). Comparisons with similar approaches in large regions worldwide, including Canada (Hird et al., 2017), the United States (Gabrielsen et al., 2016; Humphreys et al., 2017), and Asia (Peng et al., 2023), further validate the robustness and relevance of our methods and findings.

The integration of multi-temporal satellite data with machine learning, as we applied in this study, offers significant advantages for wetland modeling (Aslam et al., 2024b). Guo et al. (2017) found that most wetland studies use medium spatial resolution imagery (4–30 m), mostly Landsat images, which aligns with other *meta*-analyses of wetlands in North America (Mahdianpari et al., 2020a). Our classification demonstrated high model fit and accuracy for both wetland and non-wetland classes, highlighting its robustness across the vast and heterogeneous study area. Our model achieved an overall accuracy of 89.3 %, surpassing the 74 % to 94 % range reported in similar studies (Appendix,

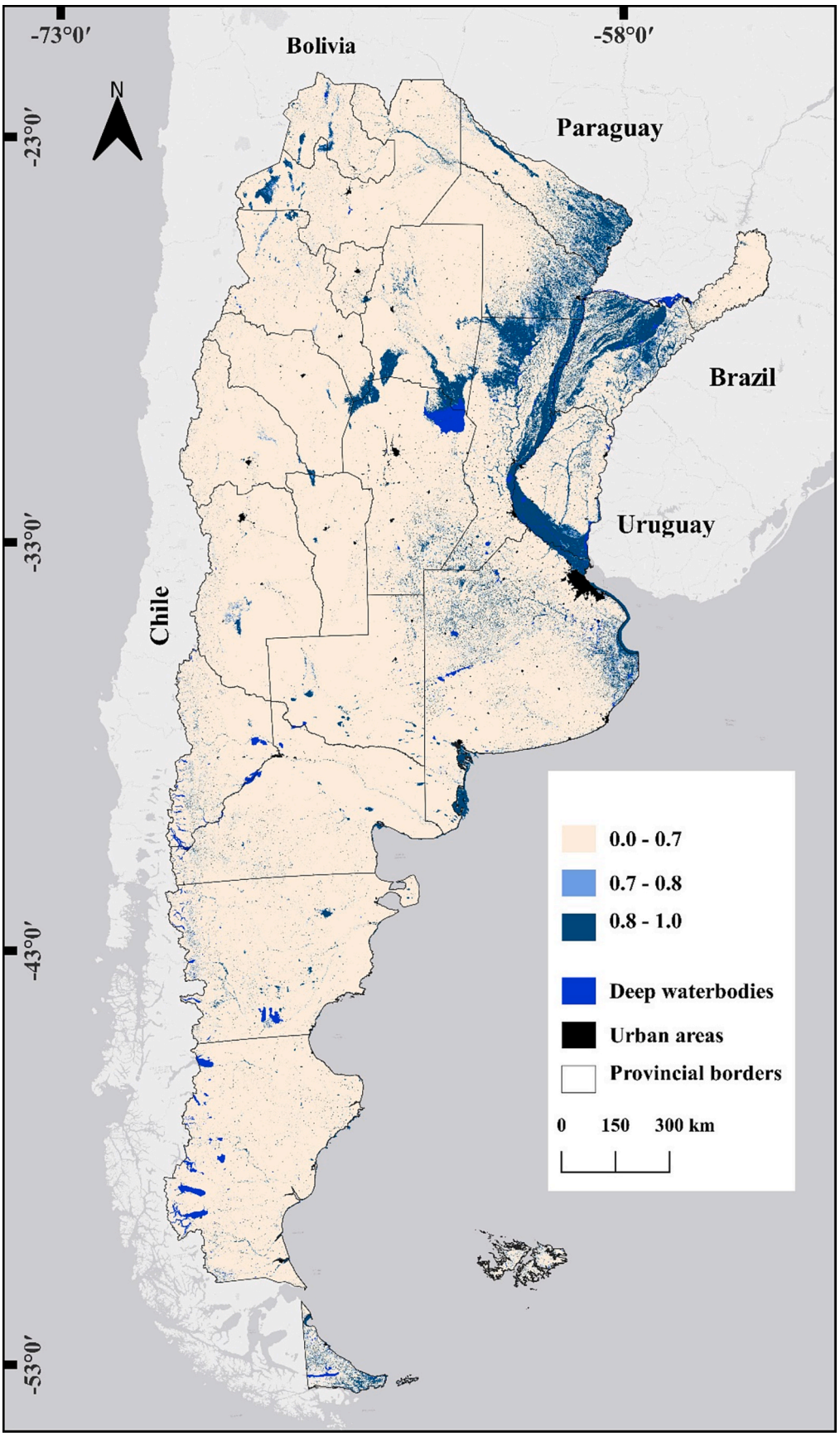


Fig. 7. Wetland occurrence probability map of Argentina, according to three probability class ranges.

Table 2
Area of wetlands according to three ranges of occurrence probability by region. Brackets indicate the wetland proportion.

Regions	Code	Probability		Total
		0.70–0.80	> 0.80	
		Surface (km^b)		
Pre-Andean mountains	1	81	655	736 (0.3 %)
Chaco	2	4,343	33,182	37,525 (14.9 %)
Puna and High-Andean Mountains	3	2,132	10,022	12,154 (4.8 %)
Misiones	4	159	696	855 (0.3 %)
Chaco-Mesopotamian river system	5	9,406	112,049	121,455* (42.6 %)
Mountain chains and valleys	6	1,001	10,124	11,125 (4.4 %)
Central Monte	7	1,504	3,993	5,497 (2.2 %)
Pampa	8	5,412	32,709	38,121 (15.2 %)
Coastal	9	1,391	11,805	13,196 (5.2 %)
Patagonia	10	6,123	19,196	25,319 (10.1 %)

* About 2,000 km^2 is attributed to rice fields cultivated at different times over the past 20 years.

Table A.2).

Multi-temporal assessment is essential for understanding wetland dynamics, as it provides a long-term perspective on wetland changes. This is particularly important given the significant impacts of global climatic events like El Niño and La Niña, on wetland ecosystems (Goodman et al., 2018), which lead to substantial fluctuations in wetland extent (Appendix, Table A.3). Our 20-year time series analysis, using a probabilistic approach, captured variability from these events and their effects on wetlands, offering insights into wetland elasticity—the ability of wetlands to respond to changes in water availability. We identified wetland areas with over 70 % probability, and our approach revealed that between 70 % and 80 % probability range, wetland elasticity becomes visible, which discrete maps cannot capture. These results underscore the critical need for multi-temporal analysis to accurately map wetlands and monitor their dynamic changes over time, aligning with findings reported by other authors such as Amani et al. (2019), Mahdianpari et al. (2020b), Onojeghuo et al. (2021), and Aslam et al. (2024b). Specifically, Aslam et al. (2024b), also used multi-temporal optical remote sensing data from 2000 to 2020 and included several spectral water indices, land cover classification, change detection, and risk mapping to examine moisture variability, land cover modifications, area changes, and proximity-based threats over two decades. By improving our understanding of how wetlands respond to varying climatic conditions through multi-temporal analysis, we can develop more effective strategies for their conservation and restoration, ensuring that these ecosystems continue to provide their valuable ecological services.

Various efforts to map Argentina's wetlands using different methodologies have led to divergent estimates of coverage. Kandus et al. (2008) estimated that 21.5 % of Argentina's surface consists of potential wetland areas, based on the National Soil Inventory (INTA, 1995) and using coarse-scale taxonomic criteria as proxies for hydric (or wetland) soils. Fabricante et al. (2022) used open spatial data from national agencies and estimated that wetlands cover 13.5 % of mainland Argentina. In contrast, our estimate approximates 9.5 %. Discrepancies arise mainly from differences in wetland definitions, data sources, and methodological approaches, particularly in incorporating water, soil, and vegetation characteristics from remote sensing data. Consistent with our findings, Gumbricht et al. (2017) estimated that 9.3 % of Argentina's surface is wetlands in their global wetland map. Although this estimate is close to ours, it excludes salt marshes and coastal wetlands and differs in wetland locations, especially in northern Argentina. Our estimate, employing a multi-temporal and probabilistic approach, provides a more accurate and detailed evaluation by utilizing recent data and finer spatial resolution.

While our research demonstrates the effectiveness of using machine learning algorithms and multi-temporal satellite imagery for wetland mapping in Argentina, it is important to acknowledge the insights of Davidson and Finlayson (2018). They point out that, despite advancements in 'top-down' remote sensing methods, these approaches often underestimate wetland areas, due to limitations in capturing the full complexity of wetlands compared to more detailed 'bottom-up' field studies. Our methodology addresses these shortcomings by integrating remote sensing data with field validation, enhancing the accuracy of our estimates in a vast and diverse country like Argentina. This approach not only improves the reliability of our wetland mapping but also illustrates the potential for more robust methodologies that leverage both remote sensing and on-the-ground data collection, thus ensuring a comprehensive understanding of wetland dynamics.

We acknowledge limitations in our approach, particularly concerning possible future updates. Differentiating irrigated crops from wetlands is challenging due to prevalent surface irrigation practices in floodplains and fluvial terraces in arid and semi-arid regions (Fig. 9a). We also recognize that overestimation of wetlands in these irrigated areas, a potential bias of our model, could influence management decisions and conservation efforts. Addressing this issue in future research, such as incorporating auxiliary datasets like land cover maps or census data, is crucial to maintaining map accuracy, as these practices increase the risk of misclassifying wetlands. To improve accuracy, future strategies should focus on refining the temporal analysis window to avoid periods of confusion and developing methods to overcome the limited accessibility to many wetlands, which complicates field data collection. Field validation is essential for ensuring classification accuracy, particularly in extensive regions like Argentina. Many studies have not validated their wetland classifications with field data (Chatziantoniou et al., 2017; Peng et al., 2023), and some have explicitly linked low accuracy to insufficient field sampling (Amani et al., 2019; Eid et al., 2020). Our approach highlights these challenges and suggests that addressing them could substantially enhance the reliability of wetland mapping efforts.

Although advancements in remote sensing have introduced high- and very high-spatial resolution sensors, such as Sentinel-2, SPOT, Quickbird, IKONOS, and Pleiades, which offer increasingly detailed imagery (from 10 m to less than 5 m) (Tine et al., 2021), these sensors still fall short for studies requiring comprehensive multitemporal analysis. Due to the absence of high-resolution imagery for the entire analysis period and the extensive geographic coverage of our study area, we relied on medium-spatial resolution Landsat sensors (TM and OLI). Moreover, while we recognize the potential benefits of SAR imagery, particularly for monitoring surface moisture and vegetation structure in wetlands, several limitations led us to prioritize optical imagery in this case. C-band SAR data from Sentinel-1, for example, faces challenges in detecting water beneath dense vegetation canopies and is also affected by terrain-induced shadows, especially in mountainous regions like the Andes. Additionally, processing SAR data can result in a loss of spatial resolution, which is critical for accurate wetland classification. The limited temporal coverage of SAR imagery during our study period further complicated its integration into a multitemporal analysis. Although SAR data was not used in this study, we incorporated two derived products (TPI, TWI) from the MDE-Ar v2.1, with a spatial resolution of 30 m and vertical accuracy of approximately 2 m (https://www.ign.gob.ar). We anticipate improvements in future studies as longer time series from newer sensors become available and plan to explore SAR integration to enhance the quality of wetland mapping.

Our approach employs state-of-the-art technologies for probabilistic wetland mapping, providing an in-depth understanding of the complexities and variations within these ecosystems. It offers comprehensive insights into temporal changes in wetland distribution, assesses human-induced impacts, and explores factors influencing wetland dynamics. As

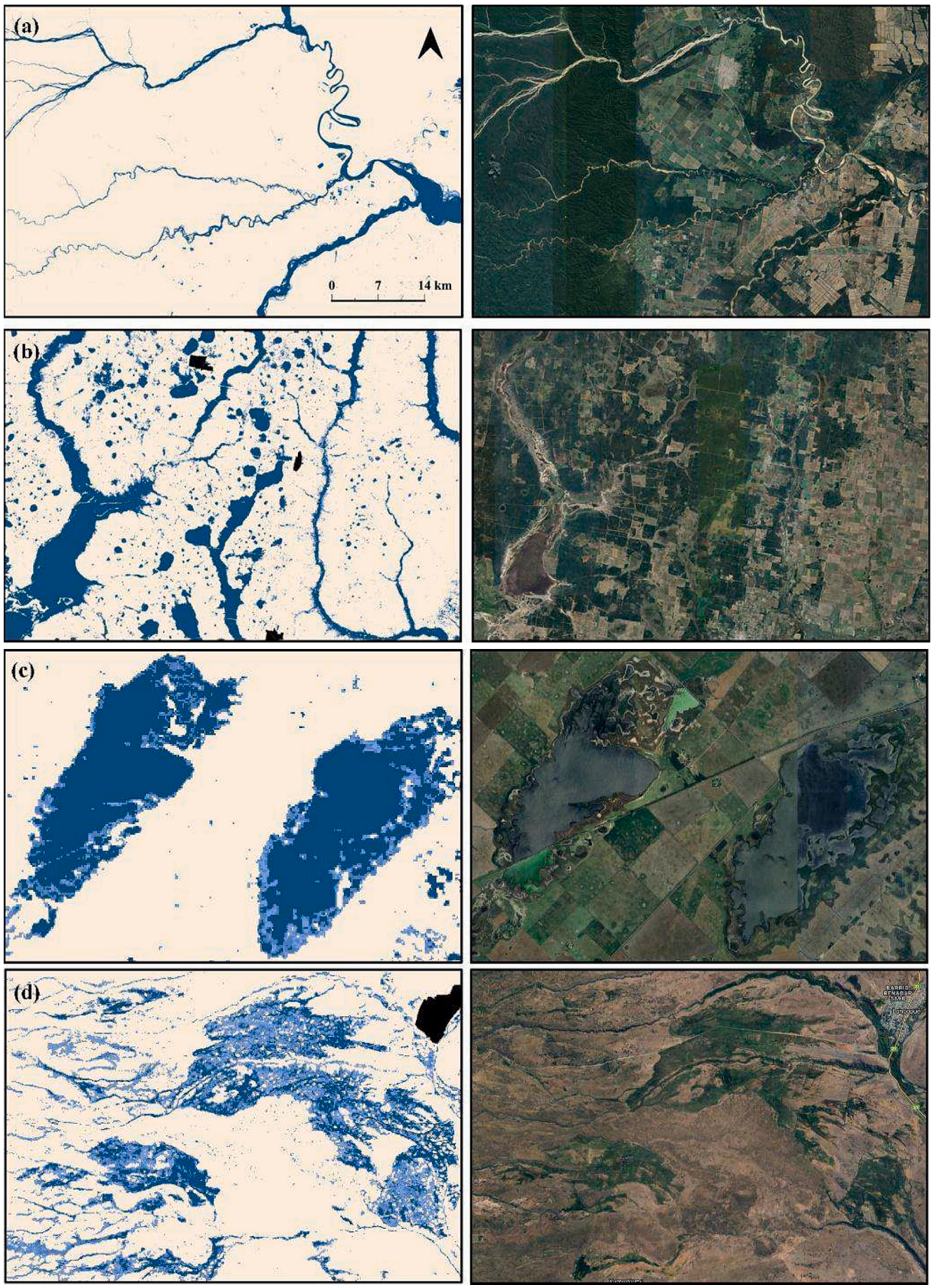


Fig. 8. Zoomed insets showcase map's visual accuracy (a-b) and successful identification of wetland elasticity zones (c-d): (a) rivers, streams, and small water bodies in NW Argentina (Region 1); (b) rivers, streams, marshes, and small water bodies in Central Pampa (Region 8); (c) shallow Pampean lakes (Region 8); and (d) mallines (wet meadows) in NW Patagonia (Region 10). All figures have the same scale bar as shown in (a).

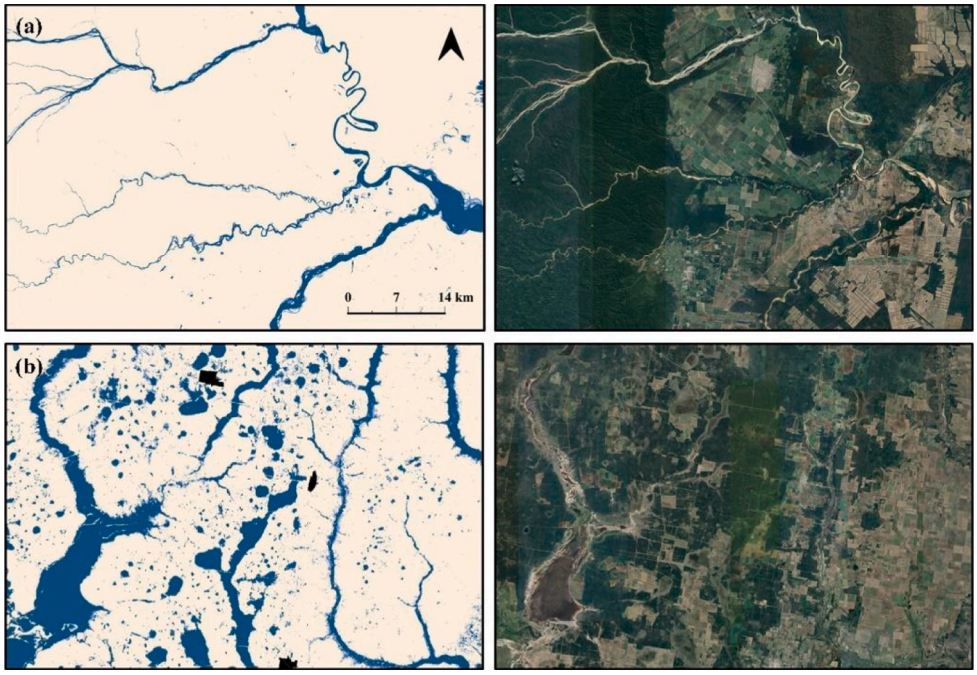


Fig. 9. Areas that exemplify challenging aspects of Argentina wetland classification (left panels), along with the corresponding high-resolution images (right panels). a) Irrigated fruit crops in the Rio Neuquén Valley (Region 7); b) Provincial Route No.5 and drainage channels running on both sides of the road (Region 5). All figures have the same scale bar as shown in (a).

technology and datasets evolve, the potential applications of this approach are expected to expand, offering researchers a robust framework for spatial analyses.

Moreover, this method holds promise across various research domains. By leveraging machine learning and multi-temporal satellite imagery, it can be adapted to efficiently map diverse land cover types or environmental phenomena with high precision. This adaptability makes it a valuable tool for studying dynamic ecosystems, such as forests, urban areas, and land use changes. It also contributes significantly to ecological studies, conservation planning, and natural resource management. Challenges include identifying stable coverages over extended periods, especially in regions with frequent land use changes like wetlands affected by drainage or new infrastructure. Addressing these challenges in future studies will enhance the effectiveness of this approach.

The accurate wetland distribution map generated through our probabilistic approach is a valuable resource for guiding land-use planning and management in Argentina. Integrating these findings into policy frameworks can improve biodiversity conservation, monitor environmental changes, and promote sustainable resource use. By delineating wetland elasticity zones and distinct characteristics, this approach provides a nuanced perspective for targeted conservation efforts and resource allocation. It significantly contributes to the Sustainable Development Goals, particularly Indicator 6.6.1, which assesses "long-term changes in the extent of water-related ecosystems".

Conclusion

Despite the ecological significance of wetlands and their increasing importance in scientific and societal contexts, they often remain underrepresented in regional and national mapping and monitoring efforts. This study demonstrates that accurate national mapping of Argentina's wetlands is achievable through the integration of multi-temporal satellite imagery, artificial intelligence techniques, and a comprehensive set of biophysical variables. Moreover, leveraging the Google Earth Engine (GEE) cloud platform has been crucial by providing access to open data and essential machine learning tools, making the study cost-effective and accessible. The probabilistic approach we adopted is particularly effective in capturing wetland dynamics that traditional methods often miss. This has led to a significant improvement in the accuracy of wetland distribution maps. The application of models such as Random Forest and logistic regression has enabled precise classification and mapping, marking a significant advancement in ecosystem cartography.

The methodology employed is spatially generalizable, temporally repeatable, and scalable, making it adaptable to various geographical and environmental contexts worldwide. The high-resolution map generated is an invaluable tool for policymakers, researchers, modelers, and stakeholders, refining ecosystem cartography and enhancing the assessment and monitoring of wetland ecosystem services. Additionally, it provides a detailed framework for analyzing spatial and temporal

dynamics. The study establishes a robust framework for forecasting future changes in wetland distribution in response to environmental factors such as climate change and infrastructure development. Integrating this map into decision-making and monitoring frameworks can address current challenges, improve conservation efforts, and ensure the sustainable management of wetlands. However, it is crucial to address certain challenges in future research, such as differentiating irrigated crops from wetlands and improving field data collection. These aspects are essential for maintaining map accuracy, especially in areas where surface irrigation practices may complicate wetland classification. Our findings underscore the importance of combining advanced mapping technologies with comprehensive biophysical indices to enhance the accuracy and utility of wetland assessments. This approach contributes to scientific understanding and global environmental management, aligning with broader conservation and sustainable development goals. The ability to capture wetland elasticity and temporal variability highlights the importance of multi-temporal analysis for effective monitoring, which will enable the development of more effective conservation and restoration strategies for these valuable ecosystems.

Furthermore, the application of our approach can extend to mapping other land cover types or environmental assessments, such as forests, urban areas, and land use changes. This versatility reinforces the method's utility in ecological studies, conservation planning, and natural resource management. Continuous advancements in technology and datasets, including the incorporation of high-resolution imagery and new sensor data, are expected to further enhance the precision and applicability of wetland mapping techniques in the future.

CRediT authorship contribution statement

María F. Navarro Rau: Writing – review & editing, Visualization, Validation, Supervision, Software. **Noelia C. Calamari:** Writing – review & editing, Writing – original draft, Validation, Supervision, Formal analysis, Conceptualization. **Carlos S. Navarro:** Writing – review & editing, Writing – original draft, Visualization, Software, Methodology, Investigation, Formal analysis, Conceptualization. **Andrea Enriquez:** Writing – review & editing, Writing – original draft, Validation, Investigation, Formal analysis. **María J. Mosciaro:** Writing – review & editing, Formal analysis, Conceptualization. **Griselda Saucedo:** Validation, Investigation, Formal analysis, Data curation. **Raul Barrios:** Validation, Investigation, Formal analysis. **Matías Curcio:** Validation, Investigation, Formal analysis. **Victorio Dieta:** Validation, Investigation, Formal analysis. **Guillermo García Martínez:** Validation, Investigation, Formal analysis. **María del R. Iturralde Elortegui:** Validation, Investigation, Formal analysis. **Nicole J. Michard:** Validation, Investigation, Formal analysis. **Paula Paredes:** Validation, Investigation, Formal analysis. **Fernando Umaña:** Validation, Investigation. **Silvina Alday:** Validation, Investigation, Formal analysis. **Alejandro Pezzola:** Validation, Investigation. **Claudia Vidal:** Validation, Investigation, Conceptualization. **Cristina Winschel:** Validation, Investigation. **Silvia Albarracin Franco:** Validation, Investigation. **Santiago Behr:** Validation, Investigation. **Francisco A. Cianfagna:** Validation, Investigation. **Maria V. Cremona:** Investigation, Conceptualization. **Fernando Alvarenga:** Validation, Investigation. **Ruth Perucca:** Validation, Investigation. **Astor Lopez:** Validation, Investigation. **Federico Miranda:** Validation, Investigation. **Ditmar B. Kurtz:** Writing – review & editing, Writing – original draft, Validation, Supervision, Methodology, Investigation, Formal analysis, Data curation.

Declaration of Competing Interest

The authors declare that they have no known competing financial interests or personal relationships that could have appeared to influence the work reported in this paper.

Acknowledgements

We sincerely thank all individuals who played a fundamental role in this study's success. Special thanks to José Volante for his valuable support and expertise in statistical analyses. Our appreciation also goes to Juan Gaitán, Gabriel Oliva, and their collaborators for sharing essential field data for validation. We acknowledge the contributions of S. Banchero, D. De Abelleyra, S. Veron, Y. Sica, M. Sepulcri, G. Gavier Pizarro, V. Utrilla, J. Zamora Gómez, and E. Livraghi in both approach discussion and other instances of the work. Lastly, we thank the editors and anonymous reviewers for their constructive comments and suggestions. This work was funded by INTA - PDI506

Appendix A. Supplementary data

Supplementary data to this article can be found online at https://doi.org/10.1016/j.wsee.2025.04.001.

References

Adam, E., Mutanga, O., Rugege, D., 2010. Multispectral and hyperspectral remote sensing for identification and mapping of wetland vegetation: a review. Wetl. Ecol. Manag. 18, 281–296. https://doi.org/10.1007/s11273-009-9169-z.

Amani, M., Salehi, B., Mahdavi, S., Granger, J., Brisco, B., 2017. Wetland classification in Newfoundland and Labrador using multi-source SAR and optical data integration. Giscience and Remote Sensing 54 (6), 779–796. https://doi.org/10.1080/15481603.2017.1331510.

Amani, M., Mahdavi, S., Afshar, M., Brisco, B., Huang, W., Mirzadeh, S.M.J., White, L., Banks, S., Montgomery, J., Hopkinson, C., 2019. Canadian Wetland Inventory using Google Earth Engine: the first map and preliminary results. Remote Sens. (basel) 11 (7), 842. https://doi.org/10.3390/rs11070842.

Aslam, R.W., Shu, H., Yaseen, A., Sajjad, A., Ul Abidin, S.Z., 2023. Identification of time-varying wetlands neglected in Pakistan through remote sensing techniques. Environ. Sci. Pollut. Res. 30, 74031–74044. https://doi.org/10.1007/s11356-023-27554-5.

Aslam, R.W., Shu, H., Javid, K., Perrvaiz, S., Mustafa, F., Raza, D., Ahmed, B., Quddoos, A., AL-Ahmadi, S., Atef Hatamleh, W., 2024a. Wetland identification through remote sensing: Insights into wetness, greenness, turbidity, temperature, and changing landscapes. Big Data Res. 35, 100416. https://doi.org/10.1016/j.bdr.2023.100416.

Aslam, R.W., Shu, H., Naz, I., Quddoos, A., Yaseen, A., Gulshag, K., Alarifi, S.S., 2024b. Machine Learning-Based Wetland Vulnerability Assessment in the Sindh Province Ramsar Site Using Remote Sensing Data. Remote Sens. (basel) 16, 92. https://doi.org/10.3390/rs16050928.

Benzaquén, L., Blanco, D.E., Bo, R., Kandus, P., Lingua, G., Minotti, P., Quintana, R. (2017). Regiones de Humedales de la Argentina. (Ministerio de Ambiente y Desarrollo Sustentable, Fundación Humedales–Wetlands International, Universidad Nacional de San Martín y Universidad de Buenos Aires: Buenos Aires, Argentina), https://www.argentina.gob.ar/sites/default/files/regioneshumedbaja2.pdf.

Berhane, T.M., Lane, C.R., Wu, Q., Autrey, B.C., Anenkhonov, O.A., Chepinoga, V.V., Liu, H., 2018. Decision-tree, rule-based, and random forest classification of high-resolution multispectral imagery for wetland mapping and inventory. Remote Sens. (basel) 10 (4), 580. https://doi.org/10.3390/rs10040580.

Beven, K.J., Kirkby, M.J., 1979. A physically based, variable contributing area model of basin hydrology. Hydrol. Sci. Bull. 24 (1), 43–69. https://doi.org/10.1080/02626667909491834.

Bey, A., Sánchez-Paus Díaz, A., Maniatis, D., et al., 2016. Collect Earth: Land Use and Land Cover Assessment through Augmented Visual Interpretation. Remote Sens. (basel) 8 (10), 807. https://doi.org/10.3390/rs8100807.

Branton, C., Robinson, D.T., 2019. Quantifying topographic characteristics of wetlandscapes. Wetlands 40, 433–449. https://doi.org/10.1007/s13157-019-01187-2.

Breiman, L., 2001. Random Forests. Mach. Learn. 45, 5–32. https://doi.org/10.1023/A:1010933404324.

Cai, W., McPhaden, M.J., Grimm, A.M., et al., 2020. Climate impacts of the El Niño-Southern Oscillation on South America. Nat. Rev. Earth Environ. 1 (4), 215–231. https://doi.org/10.1038/s43017-020-0040-3.

Canevari, P., Blanco, D.E., Bucher, E.H., Castro, G., Davidson, I.. (1999). Los Humedales de la Argentina: Clasificación, Situación Actual, Conservación y Legislación. Publication number 46, Wetlands International, Buenos Aires, Argentina.

Chander, G., Markham, B.L., Helder, D.L., 2009. Summary of current radiometric calibration coefficients for LANDSAT MSS, TM, ETM+, and EO-1 ALI sensors. Remote Sens. Environ. 113 (5), 893–903. https://doi.org/10.1016/j.rse.2009.01.007.

Chatziantoniou, A., Petropoulos, G.P., Psomiadis, E., 2017. Co-orbital Sentinel 1 and 2 for LULC Mapping with emphasis on wetlands in a Mediterranean setting based on machine learning. Remote Sens. (basel) 9, 1259. https://doi.org/10.3390/rs9121259.

Conrad, O., Bechtel, B., Bock, M., Dietrich, H., Fischer, E., Gerlitz, L., Wehberg, J., Wichmann, V., Böhner, J., 2015. System for automated geoscientific analyses

(SAGA) v. 2.1.4. Geosci. Model Dev. 8, 1991–2007. https://doi.org/10.5194/gmd-8-1991-2015.
Darrah, S., Shennan-Farpon, Y., Loh, J., et al., 2019. Improvements to the Wetland Extent Trends (WET) index as a tool for monitoring natural and human-made wetlands. Ecol. Ind. 99, 294–298. https://doi.org/10.1016/j.ecolind.2018.12.032.
Davidson, N.C., 2014. How much wetland has the world lost? Long-term and recent trends in global wetland area. Mar. Freshw. Res. 65 (10), 936–941. https://doi.org/10.1071/MF14173.
Davidson, N.C., Finlayson, C.M., 2018. Extent, regional distribution and changes in area of different classes of wetland. Mar. Freshw. Res. 69 (10), 1525–1533. https://doi.org/10.1071/MF17377.
DeLancey, E.R., Kariyeva, J., Bried, J.T., Hird, J.N., 2019. Large-scale probabilistic identification of boreal peatlands using Google Earth Engine, open access satellite data, and machine learning. PLoSONE 14 (6), e0218165. https://doi.org/10.1371/journal.pone.0218165.
De Reu, J., Bourgeois, J., Bats, M., Zwertvaegher, A., Gelorini, V., De Smedt, P., Chu, W., Antrop, M., De Maeyer, P., Finke, P., Van Meirvenne, M., Verniers, J., Crombé, P., 2013. Application of the topographic position index to heterogeneous landscapes. Geomorphology 186, 39–49. https://doi.org/10.1016/j.geomorph.2012.12.015.
Devranche, A., Poulin, B., Lefebvre, G., 2013. Mapping flooding regimes in Camargue wetlands using seasonal multispectral data. Remote Sens. Environ. 138, 165–171. https://doi.org/10.1016/j.rse.2013.07.015.
Du, Y., Zhang, Y., Ling, F., Wang, Q., Li, W., Li, X., 2016. Water bodies' mapping from Sentinel-2 imagery with Modified Normalized Difference Water Index at 10-m spatial resolution produced by sharpening the SWIR Band. Remote Sens. (basel) 8 (4), 354. https://doi.org/10.3390/rs8040354.
Eid, A.N.M., Olatubara, C.O., Ewemoje, T.A., Farouk, H., El-Hennawy, M.T., 2020. Coastal wetland vegetation feature and digital change detection mapping based on remotely sensed imagery: El-Burullus Lake Egypt. International Soil and Water Conservation Research 8 (1), 66–79. https://doi.org/10.1016/j.iswcr.2020.01.004.
Fabricante, I., Minotti, P., Kandus, P., 2022. Mapping the spatial distribution of wetlands in Argentina (South America) from a fusion of national databases. Mar. Freshw. Res. 65 (10), 934–941. https://doi.org/10.1071/MF22111.
Fluet-Chouinard, E., Stocker, B.D., Zhang, Z., et al., 2023. Extensive global wetland loss over the past three centuries. Nature 614 (7947), 281–286. https://doi.org/10.1038/s41586-022-05572-6.
Fournier, R.A., Grenier, M., Lavoie, A., Hélie, R., 2007. Towards a strategy to implement the Canadian Wetland Inventory using satellite remote sensing. Can. J. Remote. Sens. 33, 1–16. https://doi.org/10.5589/m07-051.
Gabrielsen, C.G., Murphy, M.A., Evans, J.S., 2016. Using a multiscale, probabilistic approach to identify spatial-temporal wetland gradients. Remote Sens. Environ. 184, 522–538. https://doi.org/10.1016/j.rse.2016.07.034.
Gaitán, J.J., Acuña, F., Agüero, W. et al. (2021). Cartografía del estado de degradación de las pasturas del Gran Chaco Americano. In "Informe Convenio de Asistencia Tecnica INTA-The Nature Conservancy", https://doi.org/10.13140/RG.2.2.32026.16321.
Gao, B., 1996. NDWI – a normalized difference water index for remote sensing of vegetation liquid water from space. Remote Sens. Environ. 58 (3), 257–266. https://doi.org/10.1016/S0034-4257(96)00067-3.
Gardner, R.C., Barchiesi, S., Beltrame, C., Finlayson, C.M., Galewski, T., Harrison, I., Paganini, M., Perennou, C., Pritchard, D.E., Rosenqvist, A., Walpole, M. (2015). State of the World's Wetlands and Their Services to People: A Compilation of Recent Analyses. Ramsar Briefing Note No. 7. Gland, Switzerland: Ramsar Convention Secretariat, https://doi.org/10.2139/ssrn.2589447.
Gemechu, G.F., Rui, X., Lu, H., 2021. Wetland Change Mapping Using Machine Learning Algorithms, and Their Link with Climate Variation and Economic Growth: A Case Study of Guangling County. China. Sustainability 14 (1), 439. https://doi.org/10.3390/su14010439.
Gómez-Plaza, A., Alvarez-Rogel, J., Albaladejo, J., Castillo, V., 2000. Spatial patterns and temporal stability of soil moisture across a range of scales in a semi-arid environment. Hydrol. Process. 14, 1261–1277. https://doi.org/10.1002/(SICI)1099-1085(200005)14:7<1261::AID-HYP40>3.0.CO;2-D.
Goodman, A.C., Torne, K.M., Buffington, K.J., Freeman, C.M., 2018. El Niño increases high-tide flooding in tidal wetlands along the U.S. Pacific Coast. J. Geophys. Res. Biogeo. 123 (10), 3162–3177. https://doi.org/10.1029/2018JG004677.
Gorelick, N., Hancher, M., Dixon, M., Ilyushchenko, S., Thau, D., Moore, R., 2017. Google Earth Engine: Planetary-scale geospatial analysis for everyone. Remote Sens. Environ. 202, 18–27. https://doi.org/10.1016/j.rse.2017.06.031.
Guo, M., Li, J., Sheng, C., Xu, J., Wu, L., 2017. A Review of Wetland Remote Sensing. Sensors 17 (4), 777. https://doi.org/10.3390/s17040777.
Gumbricht, T., Román-Cuesta, R.M., Verchot, L.V., Herold, M., Wittmann, F., Householder, E., Herold, N., Murdiyarso, D., 2017. An expert system model for mapping tropical wetlands and peatlands reveals South America as the largest contributor. Glob. Chang. Biol. 23 (9), 3581–3599. https://doi.org/10.1111/gcb.13689.
Gxokwe, S., Dube, T., Mazvimavi, D., 2020. Multispectral Remote Sensing of Wetlands in Semi-Arid and Arid Areas: A Review on Applications, Challenges and Possible Future Research Directions. Remote Sens. (basel) 12 (24), 4190. https://doi.org/10.3390/rs12244190.
Hird, J.N., DeLancey, E.R., McDermid, G.J., Kariyeva, J., 2017. Google Earth Engine, open-access satellite data, and machine learning in support of large-area probabilistic wetland mapping. Remote Sens. (basel) 9 (12), 1315. https://doi.org/10.3390/rs9121315.
Huete, A.R., 1988. A Soil-adjusted Vegetation Index (SAVI). Remote Sens. Environ. 25 (3), 295–309. https://doi.org/10.1016/0034-4257(88)90106-X.
Humphreys, J.M., Elsner, J.B., Jagger, T.H., Mahjoor, A., 2017. Disaggregating the Patchwork: Probabilistic models as tools to predict wetland presence as a continuous gradient. Wetlands 37, 205–219. https://doi.org/10.1007/s13157-016-0859-z.
Ilyas, S., Xu, X., Jia, G., Zhang, A., 2019. Interannual Variability of Global Wetlands in Response to El Niño Southern Oscillations (ENSO) and Land-Use. Frontiers of Earth Science 7. https://doi.org/10.3389/feart.2019.00289.
INTA-Instituto Nacional de Tecnología Agropecuaria. (1995). Atlas de suelos de la República Argentina. Buenos Aires, (UNPD project. Arg-85/019),.
Jackson, C., 2014. Wetland hydrology. In: Batzer, D., Sharitz, R. (Eds.), Ecology of Freshwater and Estuarine Wetlands, 2nd ed. University of California Press, Berkeley, pp. 43–81.
Jafarzadeh, H., Mahdianpari, M., Gill, E.W., Brisco, B., Mohammadimanesh, F., 2022. Remote Sensing and Machine Learning Tools to Support Wetland Monitoring: A Meta-Analysis of Three Decades of Research. Remote Sens. (basel) 14, 6104. https://doi.org/10.3390/rs14236104.
Junk, W.J., An, S., Finlayson, C.M., Gopal, B., Kvet, J., Mitchell, A., Mitsch, W.J., Robart, R.D., 2013. Current state of knowledge regarding the world's wetlands and their future under global climate change: a synthesis. Aquat. Sci. 75, 151–167. https://doi.org/10.1007/s00027-012-0278-z.
Kandus, P., Minotti, P., Malvarez, A.I., 2008. Distribution of wetlands in Argentina estimated from soil charts. Acta Scientiarum Biological Science, Maringá 30 (4), 403–409.
Kingsford, R.T., Basset, A., Jackson, L., 2016. Wetlands: conservation's poor cousins. Aquat. Conserv. Mar. Freshwat. Ecosyst. 26, 892–916. https://doi.org/10.1002/aqc.2709.
Mahdavi, S., Salehi, B., Granger, J., Amani, M., Brisco, B., Huang, W., 2018. Remote sensing for wetland classification: a comprehensive review. Gisci. Remote Sensing 55 (5), 623–658. https://doi.org/10.1080/15481603.2017.1419602.
Mahdianpari, M., Salehi, B., Mohammadimanesh, F., Homayouni, S., 2018. The First Wetland Inventory Map of Newfoundland Using Sentinel-1 and Sentinel-2 Data on the Google Earth Engine Cloud Computing Platform. Remote Sens. (basel) 11(1), 43, 1–27. https://doi.org/10.3390/rs11010043.
Mahdianpari, M., Granger, J.E., Mohammadimanesh, F., Salehi, B., Brisco, B., Homayouni, S., Gill, E., Huberty, B., Lang, M., 2020a. Meta-Analysis of Wetland Classification Using Remote Sensing: A Systematic Review of a 40-Year Trend in North America. Article 1882 Remote Sens. (basel) 12. https://doi.org/10.3390/rs12111882.
Mahdianpari, M., Salehi, B., Mohammadimanesh, F., Brisco, B., Homayouni, S., Gill, E., DeLancey, E.R., Bourgeau-Chavez, L., 2020b. Big Data for a Big Country: The First Generation of Canadian Wetland Inventory Map at a Spatial Resolution of 10-m Using Sentinel-1 and Sentinel-2 Data on the Google Earth Engine Cloud Computing Platform. Can. J. Remote. Sens. 46 (1), 15–33. https://doi.org/10.1080/07038992.2019.1711366.
Mainali, K., Evans, M., Saavedra, D., Mills, E., Madsen, B., Minnemeyer, S., 2023. Convolutional neural network for high-resolution wetland mapping with open data: Variable selection and the challenges of a generalizable model. Sci. Total Environ. 861, 160622. https://doi.org/10.1016/j.scitotenv.2022.160622.
Mallick, J., Talukdar, S., Shahfahad, S.P., Rahman, A., 2021. A novel classifier for improving wetland mapping by integrating image fusion techniques and ensemble machine learning classifiers. Ecology Informatics 65, 101426. https://doi.org/10.1016/j.ecoinf.2021.101426.
Mao, D., Wanga, Z., Dua, B., Lib, L., Tiana, Y., Jiaa, M., Zengc, Y., Songa, K., Jianga, M., Wangd, Y., 2020. National wetland mapping in China: A new product resulting from object based and hierarchical classification of Landsat 8 OLI images. Journal of Photogrammetry and Remote Sensing 164, 11–25. https://doi.org/10.1016/j.isprsjprs.2020.03.020.
Marton, J.M., Creed, I.F., Lewis, D.B., Lane, C.R., Basu, N.B., Cohen, M.J., Craft, C.B., 2015. Geographically isolated wetlands are important biogeochemical reactors on the landscape. Bioscience 6, 408–418. https://doi.org/10.1093/biosci/biv009.
Maxwell, A.E., Warner, T.A., Strager, M.P., 2016. Predicting palustrine wetland probability using Random Forest Machine Learning and Digital Elevation Data-derives terrain variables. Photogramm. Eng. Remote Sens. 82 (6), 437–447. https://doi.org/10.1016/S0099-1112(16)82038-8.
Melendez-Pastor, I., Navarro-Pedren, J., Gómez, I., Koch, M., 2010. Detecting drought induced environmental changes in a Mediterranean wetland by remote sensing. Appl. Geogr. 30, 254–262. https://doi.org/10.1016/j.apgeog.2009.05.006.
Mellor, A., Haywood, A., Stone, C., Jones, S., 2013. The Performance of Random Forests in an Operational Setting for Large Area Sclerophyll Forest Classification. Remote Sens. (basel) 5, 2838–2856. https://doi.org/10.3390/rs5062838.
Mitsch, W.J., Bernal, B., Nahlik, A.M., Mander, Ü., Zhang, L., Anderson, C.J., Jorgensen, S.V., Brix, H., 2013. Wetlands, carbon, and climate change. Landsc. Ecol. 28, 583–597. https://doi.org/10.1007/s10980-012-9758-8.
Mitsch, W.J., Gosselink, J.G., 2015. Wetlands, 5th ed. John Wiley, Sons Inc.
Moore, I.D., Grayson, R.B., Ladson, A.R., 1991. Digital terrain modeling: A review of hydrological, geomorphological, and biological applications. Hydrol. Process. 5 (1), 3–30. https://doi.org/10.1002/hyp.3360050103.
Natuhara, Y., 2013. Ecosystem services by paddy fields as substitutes of natural wetlands in Japan. Ecol. Eng. 56, 97–106. https://doi.org/10.1016/j.ecoleng.2012.04.026.
Neiff, J.J., Iriondo, M.H., Carignan, R. (1994). Large Tropical South American Wetlands: An Overview, p.156-165. In Anonymous (ed.). Proceedings of the International Workshop on the Ecology and Management of Aquatic-Terrestrial Ecotones, Washington DC, USA.
Neiff, J.J., 2021. Aguas continentales de Sudamérica: Biodiversidad, problemas y perspectivas. Acta Biológica Venezuelica 41, 1.
Oliva, G., Dos Santos, E., Sofía, O., Umaña, F., Massara, V., Martínez, G.G., Caruso, C., Cariac, G., Echevarría, D., Fantozzi, A., Butti, L., Bran, D., Gaitán, J., Ferrante, D.,

Paredes, P., Domínguez, E., Maestre, F.T., 2020. The MARAS dataset, vegetation and soil characteristics of dryland rangelands across Patagonia. Science Data 7, 327. https://doi.org/10.1038/s41597-020-00658-0.

Onojeghuo, A.O., Onojeghuo, A.R., Cotton, M., Potter, J., Jones, B., 2021. Wetland mapping with multi-temporal sentinel-1, -2 imagery (2017–2020) and LiDAR data in the grassland natural region of alberta. Giscience, Remote Sensing 58 (7), 999–1021. https://doi.org/10.1080/15481603.2021.1952541.

Pandey, S., Houweling, S., Krol, M., et al., 2017. Enhanced methane emissions from tropical wetlands during the 2011 La Niña. Sci. Rep. 7, 45759. https://doi.org/10.1038/srep45759.

Pekel, J.F., Cottam, A., Gorelick, N., Belward, A.S., 2016. High-resolution mapping of global surface water and its long-term changes. Nature 540, 418–422. https://doi.org/10.1038/nature20584.

Pereira, L.F., Rivadávia Mendes Oliveira, R., Kurtz, D.B., de Siqueira Castro, J., dos Santos, V. J., do Carmo Alves, S., Calijuri, M.L. (2023). Is it possible to conciliate policy-driven forestry expansion and "malezales" wetlands conservation in Argentina? Environmental Science and Policy, 142, 153-163. https://doi.org/10.1016/j.envsci.2023.02.011.

Peng, K., Jiang, W., Hou, P., Wu, Z., Ling, Z., Wang, X., Niu, Z., Mao, D., 2023. Continental-scale wetland mapping: A novel algorithm for detailed wetland types classification based on time series Sentinel -1/2 images. Ecol. Ind. 148, 110113. https://doi.org/10.1016/j.ecolind.2023.110113.

Qu, Y., Zeng, X., Luo, C., Zhang, H., Ni, H., 2023. Prediction of wetland biodiversity pattern under the current land-use mode and wetland sustainable management in Sanjiang Plain. China. Ecological Indicators 147, 109990. https://doi.org/10.1016/j.ecolind.2023.109990.

Ramsar Convention on Wetlands. (1971). Convention on Wetlands of International Importance Especially as Waterfowl Habitat. Final Text adopted by the International Conference on the Wetlands and Waterfowl at Ramsar, Iran, 2 February 1971, Iran, https://www.ramsar.org/sites/default/files/documents/library/original_1971_convention_e.pdf., 1971.

Ramsar Convention on Wetlands. (2012). 11th Meeting of the Conference of the Parties to the Convention on Wetlands: Wetlands home and destination. Resolution XI.15, Bucharest, 6-12 July.

Ramsar Convention on Wetlands. (2018). Global Wetland Outlook: State of the World's Wetlands and their Services to People. Gland, Switzerland: Ramsar Convention Secretariat.

Shafi, A., Chen, S., Waleed, M., Sajjad, M., 2023. Leveraging machine learning and remote sensing to monitor long-term spatial-temporal wetland changes: towards a national RAMSAR inventory in Pakistan. Appl. Geogr. 151, 102868. https://doi.org/10.1016/j.apgeog.2022.102868.

Simioni, J.P.D., Guasselli, L.A., de Oliveira, G.G., Ruiz, L.F.C., de Oliveira, G., 2020. A comparison of data mining techniques and multi-sensor analysis for inland marshes delineation. Wetl. Ecol. Manag. 28, 577–594. https://doi.org/10.1007/s11273-020-09731-2.

Souza, C.M., Kirchhoff, F.T., Oliveira, B.C., Ribeiro, J.G., Sales, M.H., 2019. Long-term annual surface water change in the Brazilian Amazon Biome: potential links with deforestation, infrastructure development and climate change. Water 11 (3), 566. https://doi.org/10.3390/w11030566.

Tang, Z., Li, Y., Gu, Y., Jiang, W., Xue, J., Hu, Q., LaGrange, T., Bishop, A., Drahota, J., Li, R., 2016. Assessing Nebraska playa wetland inundation status during 1985–2015 using Landsat data and Google Earth Engine. Environ. Monit. Assess. 188, 654. https://doi.org/10.1007/s10661-016-5664-x.

Tine, D., Faye, G., Marico, O., Mbaye, M., Biaye, L., Faye, M., Faye, G., 2021. Contribution of Sentinel-2/Landsat-8 OLI Images to Extracting Vegetation Cover and Wetlands Area in Urban Zones: Case of the Dakar Region (Senegal). J. Geogr. Syst. 13, 523–537. https://doi.org/10.4236/jgis.2021.134029.

Tiner, R.W., Lang, M.W., Klemas, V.V. (2015). Remote Sensing of Wetlands: Applications and Advances. (1st ed.). CRC Press. Boca Raton, FL (574 pp) https://doi.org/10.1201/b18210.

Townshend, J.R.G., Justice, C.O., 1986. Analysis of the Dynamics of African Vegetation Using the Normalized Difference Vegetation Index. Int. J. Remote Sens. 8, 1189–1207. https://doi.org/10.1080/01431168708954764.

Watanabe, T. (2018). Paddy fields as artificial and temporal wetlands. In G. Ondrašek (Eds.), Irrigation in agroecosystems.

Whiteside, T.G., Bartolo, R.E., 2015. Mapping aquatic vegetation in a tropical wetland using high spatial resolution multispectral satellite imagery. Remote Sens. (basel) 7 (9), 11664–11694. https://doi.org/10.3390/rs70911664.

Xu, H., 2006. Modification of Normalized Difference Water Index (NDWI) to enhance open water features in remotely sensed imagery. Int. J. Remote Sens. 27, 3025–3033. https://doi.org/10.1080/01431160600589179.

Zhuang, Y., Liu, H., Zhang, L., Li, S., 2020. Research perspectives on paddy field systems: ecological functions and environmental impacts. Int. J. Agric. Sustain. 18 (6), 505–520. https://doi.org/10.1080/14735903.2020.1793652.